

GazeMoDiff: Gaze-guided Diffusion Model for Stochastic Human Motion Prediction

Haodong Yan*
Xi'an Jiaotong University

Zhiming Hu†
University of Stuttgart

Syn Schmitt‡
University of Stuttgart

Andreas Bulling§
University of Stuttgart

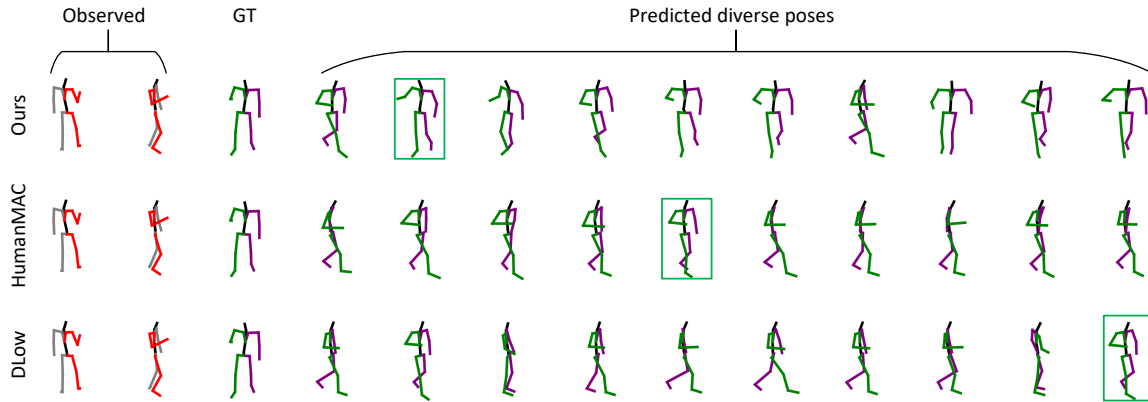


Figure 1: Motions in the future one second generated from different methods on the MoGaze dataset [33] with best prediction boxed in green. Our method can generate human motions that are more close to the ground truth (GT) than other methods.

ABSTRACT

Human motion prediction is important for virtual reality (VR) applications, e.g., for realistic avatar animation. Existing methods have synthesised body motion only from observed past motion, despite the fact that human gaze is known to correlate strongly with body movements and is readily available in recent VR headsets. We present *GazeMoDiff* – a novel gaze-guided denoising diffusion model to generate stochastic human motions. Our method first uses a graph attention network to learn the spatio-temporal correlations between eye gaze and human movements and to fuse them into cross-modal gaze-motion features. These cross-modal features are injected into a noise prediction network via a cross-attention mechanism and progressively denoised to generate realistic human full-body motions. Experimental results on the MoGaze and GIMO datasets demonstrate that our method outperforms the state-of-the-art methods by a large margin in terms of average displacement error (15.03% on MoGaze and 9.20% on GIMO). We further conducted an online user study to compare our method with state-of-the-art methods and the responses from 23 participants validate that the motions generated by our method are more realistic than those from other methods. Taken together, our work makes a first important step towards gaze-guided stochastic human motion prediction and guides future work on this important topic in VR research.

Index Terms: Human-centered computing—Human computer interaction—Interaction paradigms—Virtual reality; Computing methodologies—Machine learning—Machine learning approaches—

*e-mail: k610215095@stu.xjtu.edu.cn

†e-mail: zhiming.hu@vis.uni-stuttgart.de

‡e-mail: schmitt@simtech.uni-stuttgart.de

§e-mail: andreas.bulling@vis.uni-stuttgart.de

Neural networks;

1 INTRODUCTION

Generating realistic human body movements is a key research challenge in the area of virtual reality (VR) and is the basis for safe, smooth, and immersive human-environment [12] and human-human interactions [22, 29]. Human motion prediction (HMP) enables a number of exciting applications, such as redirected walking to create the illusion of unlimited virtual interaction spaces [3, 53] or to steer users away from physical boundaries, such as walls, and thus avoid collisions [17, 66]. Human motion prediction can also provide users with a low-latency experience by preparing VR content in advance based on the predicted future human poses [9, 23] and it has been used to generate human-like motions for virtual agents to enhance the interaction experience [6, 14].

Previous work on HMP has typically generated human motions in a deterministic way, i.e. by producing only a single prediction at a time [7, 8, 19, 41]. Recently, in light of the fact that human motion is stochastic by nature [4, 10], researchers have turned to stochastic human motion prediction, i.e. generating a number of reasonable human motions at a time [4, 5, 10, 62]. Stochastic human motion prediction suits the needs of many VR applications. For example, to minimise the collision risk in a virtual environment, it is necessary to consider multiple possible future trajectories to warn the users. To produce realistic virtual agents, it is also beneficial to synthesise diverse human motions that users can peruse and select from according to their personal preferences. However, existing stochastic HMP methods typically generate human motions using only past observed motions and neglect other modalities, in particular human eye gaze. With rapid advances in eye tracking technology, human eye gaze information has become readily available in many VR head mounted displays (HMDs), such as HTC Vive Pro Eye, Varjo VR-3, and Vision Pro, and has demonstrated its potential for gaze-based interaction [50] and gaze-contingent rendering [26, 27] in VR. In addition, a large body of work in the cognitive sciences and human-centred computing has shown that human body movements

are closely coordinated with human gaze behaviour [24, 25, 49]. Despite this close coordination, information on eye gaze has not been used for stochastic human motion prediction so far.

To address this limitation we propose *GazeMoDiff*¹ – the first **Gaze**-guided human **Motion Diffusion** model to generate realistic and diverse human motions. At the core of our method is a spatio-temporal graph attention network (ST-GAT) that models the correlations between eye gaze and different body joints across each time step and fuses them into cross-modal gaze-motion features. The gaze-motion features are then injected into a noise prediction network via a cross-attention mechanism to generate realistic and diverse human motions through progressive denoising. We report extensive evaluations of our method using common metrics for stochastic HMP and visualisation analysis on two public datasets: MoGaze [33] and GIMO [66]. We show that our method significantly outperforms state-of-the-art methods by 15.03% on MoGaze and 9.20% on GIMO in terms of average displacement error, and 15.24% on MoGaze and 8.92% on GIMO in final displacement error. To evaluate the realism of the motions generated by our method, we further perform an on-line user study to compare the performances of different methods by human intuition. The 414 responses from 23 participants demonstrate that our method can generate motions that are more realistic than the state of the art.

The main contributions of our work are three-fold:

- We propose a novel gaze-guided diffusion model for stochastic HMP: Our model first extracts cross-modal gaze-motion features using a ST-GAT, and then injects these features into a noise prediction network via a cross-attention mechanism, and finally generates diverse human motions through progressive denoising.
- We provide extensive evaluations of our method using common metrics for stochastic HMP and visualisation analysis on two publicly available benchmarks and show that our method significantly outperforms the state-of-the-art methods.
- We perform an on-line user study for subjective assessment and the responses from 23 participants validate that the motions generated by our method are more realistic than that from other methods.

2 RELATED WORK

2.1 Human Motion Prediction

Human motion prediction is a fundamental research topic in virtual reality (VR). Early studies commonly considered HMP as a deterministic sequence prediction task, tackling it with recurrent neural networks (RNN) [16, 18, 37, 41], graph neural networks (GNN) [35, 36] and Transformers [1, 42]. Noticing that human motion trends are inherently stochastic, recent works began to predict human motions in a stochastic way using generative models such as variational autoencoder (VAE) [2, 39], generative adversarial network (GAN) [5, 28, 34], and Flow networks [62]. Generative approaches model motion possible distribution rather than a single trajectory. It meets the demands of many VR applications such as collision warning during human-human interaction and human-environment interaction. These methods often design diversity-aware loss or sampling [39, 62] to enforce diversity. However, the predicted sequences were not plausible. Recently, the emergence of the denoising diffusion model [20], which has shown both diversity and realism in generalisation in the fields of image generation [43, 45, 64] without any explicit diversity constraints. Several works [4, 10, 48] have applied diffusion in the field of stochastic motion prediction and have achieved more realistic results. However, those methods only generate predictions based on observed poses and neglect other potentially

Diffusion process: Transfer clean sample into pure noise by adding Gaussian Noise

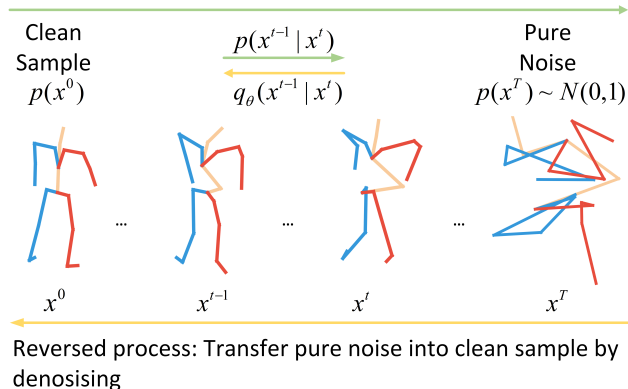


Figure 2: Diffusion process and reversed process in DDPM.

exploitable information in VR scenarios from other modalities. To fill this gap, our work introduces a naturally available modal, gaze, into a diffusion-based model for the first time.

2.2 Correlations between Eye Gaze and Body Motions

Intuitively, a period of gaze information seems related to intention [31], which can drive future motion trends. Extensive work in cognitive science and the human-computer interaction has also demonstrated this correlation between gaze and subsequent motion. Some research [27, 32, 63] have shown that in many everyday activities, such as free viewing or object searching, head movements are closely associated with eye movements. Emery et al. [15] focused on how eye, hand, and head movements coordinate in a virtual world, and then leveraged that coordination to enhance gaze estimation. Sidenmark et al. [49, 51] also have revealed the coordination of eye, head and torso movements during gaze shifts in VR.

Although the aforementioned works have indicated the strong relationship between eye movements and human motion trends, existing stochastic HMP methods have not considered this correlation yet. We are the first to leverage the correlation between gaze and motion, which enhances the realism and trustworthiness of stochastic HMP. This gaze-motion correlation ultimately leads to superior quantitative performance, as we show in this work.

2.3 Denoising Diffusion Models

Denoising Diffusion Models, or more precisely, Denoising Diffusion Probabilistic Models (DDPM) [13, 20, 47, 52] are a group of the most ingenious generative models. They aim to model reversing a Markov chain of the diffusion process illustrated in Fig. 2. During training, noisy samples are obtained by incrementally adding noise to raw samples. The DDPM model then progressively reverses the diffusion process by predicting noise and denoising the samples. The loss is computed as the difference between predicted noise and Gaussian noise added during the diffusion process. In the inference stage, given a well-trained DDPM, it can generate diverse samples from a Gaussian distribution via the reversed diffusion process.

Owing to the power of generating diverse and high-quality samples, these models have been applied in image/video generation [21, 47], anomaly detection [60], objection detection [11], 3D reconstruction [61], time series forecasting [46] and imputation [54]. In a similar context, Tevet et al. [55] proposed a text-driven human motion synthesis method with diffusion models. Recently, Barquero et al. [4] utilised a latent diffusion model to sample the diverse behaviour code to predict stochastic motions. Chen et al. [10]

¹Code and pretrained models will be released upon acceptance

presented an end-to-end motion prediction framework based on diffusion models without complicated loss constraints and training processes. Their work has demonstrated competitive performance in this domain. Although these diffusion-based methods have made significant contributions to stochastic HMP, unrealistic results can be yielded by only focusing on past human poses and neglecting other important information from other modalities. To address these problems, our gaze-guided diffusion model takes into account the coordination between gaze and human movements. By incorporating gaze information, we aim to generate more reasonable and plausible human motion predictions. This integration of gaze and human movement data allows for a more holistic understanding of human behaviour, resulting in improved motion synthesis that better aligns with intentions.

3 THE GAZEMODIFF MODEL

Our diffusion model for gaze-guided stochastic human motion forecasting takes past body poses and gaze information as input. We encode the human pose $p \in \mathbb{R}^{j \times 3}$ using the 3D positions of all human joints, where j denotes the number of human joints. Gaze $g_i \in \mathbb{R}^{1 \times 3}$ is defined as the unit direction vector. Given a H -frame observed sequence $\mathbf{x} = [(g_1, p_1), (g_2, p_2), \dots, (g_H, p_H)]$, our goal is to train a model that can predict k different following F -frame future human motions. It can be formulated as $\mathbf{P} = f_p(\mathbf{x}, k)$, where $\mathbf{p} = \{\mathbf{p}_0, \mathbf{p}_1, \dots, \mathbf{p}_k\}$ and $\mathbf{p}_i = [p_{H+1}, p_{H+2}, \dots, p_{H+F}]$. An overview of our model is shown in Fig. 3. At a high level, our model consists of a cross-modal fusion module to fuse human gaze and full body poses as well as a motion generation module.

3.1 Gaze-motion Fusion

Recent works have demonstrated that a graph structure is a particularly effective representation to learn abstract correlations between body joints [35, 36, 38]. We treated gaze as a ‘‘virtual joint’’ and combined gaze and poses together as a fully connected spatial-temporal graph $X \in \mathbb{R}^{3 \times (j+1) \times (H+F)}$, where later F -frame poses were padded with the last observed frame.

We further employed an approximate discrete cosine transform (DCT) [39] that selected the first L components. By leveraging this transformation, the time dimension was reduced to L from $H + F$, which both improved the smoothness of generation and reduced computational complexity [40]. Given the original spatial-temporal graph $X \in \mathbb{R}^{3 \times (j+1) \times (H+F)}$, the DCT spatial-temporal graph $Y \in \mathbb{R}^{3 \times (j+1) \times L}$ was obtained by DCT.

Previous work on graph attention networks (GATs) has shown good results for human pose aggregation [57]. We designed the Gaze-motion Fusion module *GazePoseFuse*(\cdot), illustrated in Fig. 3, to model the spatio-temporal correlations in the defined graph and fuse the gaze-motion features. The Gaze-motion Fusion module was composed of a stack of temporal GAT layers and spatial attention GAT layers with skip connections. In this module, the number of middle blocks m is 4 and there is a layer normalisation, tanh activation function and a dropout layer after each middle block. The attention head of each spatial GAT layer and temporal GAT layer is 8. The output feature dimension of the start, middle, and end block is 16, 16, and 3, respectively. The gaze-motion feature is calculated as:

$$H'' = \text{GazePoseFuse}(Y) \quad (1)$$

Given the input $H \in \mathbb{R}^{f \times (j+1) \times L}$ of each block, where f is the feature dimension of input, we first aggregated features along the temporal dimension and obtain $H' = [h'_1, h'_2, \dots, h'_L] \in \mathbb{R}^{f \times (j+1) \times L}$ in the following way:

$$h'_i = \text{LeakyReLU} \left(\frac{1}{N_{\text{head}}} \sum_{n=1}^{N_{\text{head}}} \sum_{k=1}^L \alpha_{ik}^n h_k \right) \quad (2)$$

where $h'_i \in \mathbb{R}^{f \times (j+1)}$ is the output feature of node i , h_k is the input feature of node k , and N_{head} denotes the number of heads for attention. We fused different output features from each head by averaging them. For each head, the attention matrix α_{ik}^n represents interactions between each timestamp, calculated as follows:

$$\alpha_{ik}^n = \frac{\exp(\text{LeakyReLU}(\mathbf{a}^n [h_i \oplus h_k]))}{\sum_{l=1}^T \exp(\text{LeakyReLU}(\mathbf{a}^n [h_i \oplus h_l]))} \quad (3)$$

where \mathbf{a}^n is a parameter vector $\in \mathbb{R}^{2f(j+1) \times 1}$

A weigh matrix $\mathbf{W} \in \mathbb{R}^{f \times f'}$ was then used to transfer feature dimension from $H' \in \mathbb{R}^{f \times (j+1) \times L}$ to $\tilde{H}' \in \mathbb{R}^{f' \times (j+1) \times L}$.

To further capture correlations between joints and the gaze feature, we proposed a spatial graph attention network layer. Specifically, the spatial GAT layer was in a similar manner to the temporal GAT layer, differing primarily in how attention coefficients were computed. Rather than aggregating along the temporal axis as in the temporal GAT, the spatial GAT aggregated features across spatial dimensions as follows:

$$h''_i = \text{LeakyReLU} \left(\frac{1}{\tilde{N}_{\text{head}}} \sum_{n=1}^{\tilde{N}_{\text{head}}} \sum_{k=1}^{j+1} \tilde{\alpha}_{ik}^n \tilde{h}'_k \right) \quad (4)$$

where $h''_i \in \mathbb{R}^{f' \times L}$ is the output feature of node i and \tilde{N}_{head} denotes the number of heads for attention. We also applied an average function to fuse different output features from each head in spatial GAT. For each head, the attention matrix $\tilde{\alpha}_{ik}^n$ represents interactions between each timestamp, calculated as follows:

$$\tilde{\alpha}_{ik}^n = \frac{\exp(\text{LeakyReLU}(\tilde{\mathbf{a}}^n [\tilde{h}'_i \oplus \tilde{h}'_k]))}{\sum_{l=1}^{j+1} \exp(\text{LeakyReLU}(\tilde{\mathbf{a}}^n [\tilde{h}'_i \oplus \tilde{h}'_l]))} \quad (5)$$

where $\tilde{\mathbf{a}}^n$ is a parameter vector $\in \mathbb{R}^{2f' L \times 1}$

3.2 Motion Generation

We formulated the motion generation task as an inverse diffusion process, which contains iterative noise prediction and denoising steps.

Noise prediction. Inspired by text-driven noise prediction network [65], we designed a noise prediction network ε_θ . This network is developed to predict the noise at the current time step given the gaze-motion features H'' and noisy motion sequence $Y^t \in \mathbb{R}^{3 \times (j+1) \times L}$ from the previous time step. As illustrated in Fig. 3, ε_θ consists of n stacked self-attention block, cross-attention block and multilayer perceptron(MLP) block with skip connections. The predicted noise at time step t is formulated as follows:

$$\bar{\varepsilon} = \varepsilon_\theta(Y^t, H'', t) \quad (6)$$

To capture more complex representations and better model the temporal correlations within the noisy gaze-motion sequence $Y^t \in \mathbb{R}^{3 \times (j+1) \times L}$, we first employed a linear transformation to project the sequence into a higher-dimension latent space $Y^t \in \mathbb{R}^{3 \times (j+1) \times L'}$. We then apply an efficient self-attention block [65] to further model temporal correlations between each frame:

$$\mathbf{Y} = \text{Dropout} \left(\text{softmax}(\mathbf{Q}) \text{softmax}(\mathbf{K}^\top) \right) \text{LN}(\mathbf{V}) + Y^t \quad (7)$$

where LN is layer normalisation, $\mathbf{Q} \in \mathbb{R}^{L \times d}$, $\mathbf{K} \in \mathbb{R}^{L \times d}$, and $\mathbf{V} \in \mathbb{R}^{L \times d}$ are calculated using the original self-attention mechanism [56]:

$$\mathbf{Q} = \mathbf{W}_q Y^t, \mathbf{K} = \mathbf{W}_k Y^t, \mathbf{V} = \mathbf{W}_v Y^t \quad (8)$$

where \mathbf{W}_q , \mathbf{W}_k and \mathbf{W}_v are learnable parameter matrices.

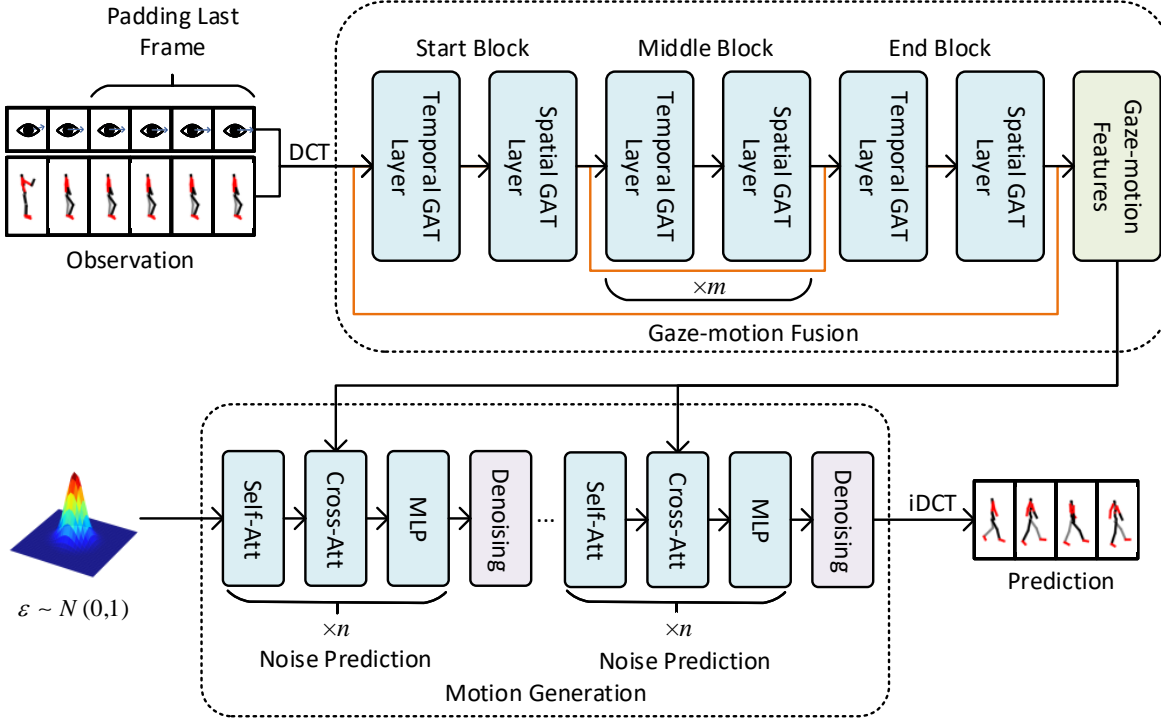


Figure 3: Overview of the proposed method *GazeMoDiff*. *GazeMoDiff* first uses a spatio-temporal graph attention network to extract and fuse features from eye gaze and human motions, then injects these features into a noise prediction module via a cross-attention mechanism, and finally generates diverse human motions through progressive denoising.

We then applied a step hint module to inform about how many steps of noise have been added thus far. We first obtained the timestep embedding \mathbf{e}_t using position embedding [56]. The gaze-motion historical features H'' were also fused with a learned linear projection of the timestep embedding, $\mathbf{e} = \mathbf{e}_t + \mathbf{W}'H''$. This fused embedding \mathbf{e} was then injected into the output of the self-attention block using a feature-wise linear modulation:

$$w = \phi_w(\psi(\mathbf{e}_t)), b = \phi_b(\psi(\mathbf{e}_t)), \mathbf{Y}' = \text{SiLU}(w \cdot \mathbf{Y} + b) \quad (9)$$

where (\cdot) denotes element-wise multiplication, ϕ_w and ϕ_b are linear projections, and ψ is a single layer MLP with SiLU activation function. This modulation allowed the step hint embedding to influence the self-attention features. We also applied this block after each cross-attention and MLP block, enabling the timestep embedding to provide hints throughout the network.

To incorporate the historical gaze-motion features H'' and leverage their impact on noise prediction, we utilised cross-attention blocks. These blocks enable a deeper exploration of how the historical features influence the noise predictions at different denoising steps. In addition, computing the contributions of different attention heads in parallel better integrates information from both modalities (gaze and motion) from multiple perspectives. Potentially, the noisy motions can also provide feedback to update H'' , leading to a collaborative learning process. In the cross-attention block, \mathbf{Q}_c and \mathbf{V}_c were calculated by gaze-motion historical features H'' while \mathbf{K}_c was calculated by the output of self-attention block \mathbf{Y}' . The output of the

cross-attention block was calculated as follows:

$$\mathbf{Y}_c = \text{Dropout}\left(\text{softmax}(\mathbf{Q}_c)\text{softmax}(\mathbf{K}_c^\top)\right)\text{LN}(\mathbf{V}_c) + \mathbf{Y}' \quad (10)$$

$$\mathbf{Q}_c = \mathbf{W}'_q H'', \mathbf{K}_c = \mathbf{W}'_k \mathbf{Y}', \mathbf{V}_c = \mathbf{W}'_v H'' \quad (11)$$

Finally, we employed a two-layer MLP with GELU activation function and dropout to further extract features. An output projection layer was added at the end to align with the noise dimension.

In our implementation, the noise prediction network contained 4 self-attention blocks, 4 cross-attention blocks, and 4 MLP blocks. Each attention operation used 8 attention heads. The timestep embedding dimension and the latent space dimension were both set to 512.

Denoising. In a vanilla approach, the denoised sequence was generated directly from the Gaussian noise input. However, due to the accumulation of prediction noise errors, the information of observation in the padded sequence is far away from the truth in the latter steps. In each denoising step, the observed sequence was also available to guide the generation in the original space. Thus, we employed an ingenious prediction mask mechanism [10]:

$$Y^{t-1} = \text{DCT}\left(\mathbf{M} \odot \text{iDCT}\left(Y_{orig}^{t-1}\right) + (\mathbf{1} - \mathbf{M}) \odot \text{iDCT}\left(Y_{pred}^{t-1}\right)\right) \quad (12)$$

where $\mathbf{M} = \underbrace{[1, 1, \dots, 1, 0, 0, \dots]}_H \in \mathbb{R}^{(H+F) \times 1}$ is a mask vector indicating which frames are observed. Y_{orig}^{t-1} is obtained by adding

$t - 1$ iterations of Gaussian noise, and Y_{pred}^{t-1} is obtained by denoising the output Y^t from the previous iteration:

$$Y_{orig}^{t-1} = \sqrt{\tilde{\beta}_{t-1}}Y + \sqrt{1 - \tilde{\beta}_{t-1}}\varepsilon, \tilde{\beta}_t = \prod_{i=1}^t \beta_i, \beta_i \in [0, 1] \quad (13)$$

$$Y_{pred}^{t-1} = \frac{1}{\sqrt{\beta_t}} \left(Y^t - \frac{1 - \beta_t}{\sqrt{1 - \tilde{\beta}_t}} \varepsilon_\theta(Y^t, H'', t) \right) + (1 - \beta) \varepsilon \quad (14)$$

where t denotes the t -th noise iteration, β_t controls noise level, and $\varepsilon \sim N(0, I)$. At the start, Y^t is sampled from Gaussian noise.

Through this iteration process, we can obtain the full generated sequence $\hat{\mathbf{p}} = \text{iDCT}(Y^0)$. The last H frames were predicted motions.

The detailed inference procedure is illustrated in the supplementary material.

3.3 Training

In the training stage, the observation and prediction sequences are both available. Thus, we trained the model on the full-motion sequence $X_{full} \in \mathbb{R}^{3 \times (j+1) \times (H+F)}$ without pre-padding. First, we also transfer into the DCT space $Y_{full} \in \mathbb{R}^{3 \times (j+1) \times L}$. We then add noise to Y_{full} to generate a noisy sequence Y_{full}^t via Equation 13. Then we predict the noise through Equation 1 and Equation 6

We then optimised all parameters in our pipeline by minimising the l_2 loss between the predicted noise $\varepsilon_\theta(Y^t, H'', t)$ and true noise ε :

$$\mathcal{L} = \mathbb{E}_{\varepsilon, t} \left[\left\| \varepsilon - \varepsilon_\theta(Y_{full}^t, H'', t) \right\|^2 \right] \quad (15)$$

The detailed training procedure is shown in the supplementary material.

4 EXPERIMENTS

4.1 Datasets

Only a limited number of datasets contain synchronised recordings of both eye gaze and full-body human motion. We evaluated our method on two such public datasets: MoGaze [33] and GIMO [66].

MoGaze. The MoGaze dataset provides motion capture and eye-tracking data recorded simultaneously from 6 participants performing *place* and *pick* actions. It contains over 3 hours of movement and gaze recordings captured at 30 Hz. The pose of the human body is expressed using 3D coordinates and Euler angles of 21 joints, while the gaze is represented as a direction vector. Following prior work [4, 10, 62] on stochastic HMP, we represented the pose using only the 3D coordinates of each joint. The gaze vector was treated similarly to a virtual joint, with coordinates computed as the vector sum of the head joint coordinates and the gaze direction vector. This unified representation of both pose and gaze solely in joint coordinate space allowed us to apply existing stochastic models to compare easily. Without special notes, all *baselines + gaze* donate to this implementation. Pose sequences from $p1$, $p2$, $p4$, $p5$, and $p6$ were used for training while that from $p7$ was used for testing.

GIMO. The GIMO dataset contains motion and gaze data captured from 11 participants. The action categories include *sitting* or *laying on objects*, *touching*, *holding*, *reaching to objects*, *opening*, *pushing*, *transferring*, *throwing*, *swapping objects*, etc. The skeletal model consists of 23 joints. As with MoGaze, we represented the pose using only the 3D coordinates of each GIMO skeleton joint, and the gaze was represented as a direction vector. To enable training and evaluation, we followed the official dataset splits in GIMO [66]. The training set comprises motion and gaze recordings from 12 scenes, while the test set contains data from 14 scenes,

including 12 known environments and 2 new, unseen environments. This evaluation protocol allows the assessment of generalisation capabilities to novel scenes.

4.2 Evaluation Metrics

To evaluate the performance of our model, we employed five commonly used metrics following prior stochastic HMP works [4, 10, 62].

Average Pairwise Distance (APD) measures diversity as the average L2 distance between all motion examples generated by the model. Higher APD indicates more diverse predictions.

Average Displacement Error (ADE) and **Final Displacement Error (FDE)** measure accuracy. ADE is the average L2 distance between ground truth and predicted motions over the whole future sequence. FDE is the L2 distance at the final timestep. Lower ADE and FDE indicate more accurate predictions.

Multi-Modal Average Displacement Error (MMADE) and **Multi-Modal Final Displacement Error (MMFDE)** are metrics specifically designed to handle the multi-modal nature of predictions in stochastic HMP tasks. These metrics take into account the fact that there can be multiple plausible ground truth sequences for a given input. The multiple plausible ground truth sequences are obtained by clustering similar past motions. Lower MMADE and MMFDE indicate a better ability to generate multi-modal predictions.

4.3 Baselines

We compared our approach with the following state-of-the-art methods in stochastic HMP.

- *DLow* [62]: *DLow* is a latent flow-based model to generate diverse motion via diversity-promoting sampling and loss.
- *CVAE* [62]: *CVAE* is a conditional variational autoencoder utilised in *DLow* [62] as a pre-trained generative model which can also forecast stochastic motions.
- *BeLFusion* [4]: *BeLFusion* is a latent diffusion-based model to predict diverse motion benefited from disentangling the behavioural representation from past poses and motions.
- *HumanMac* [10]: *HumanMac* is an end-to-end single-loss stochastic HMP model with a DCT Completion fashion in the inference.

4.4 Implementation Details

We set the observation and prediction time window to 0.5 seconds (15 frames) and 2 seconds (60 frames) for both the MoGaze and GIMO datasets, following common practices in stochastic human motion prediction tasks. [4, 10, 62] As baselines are not evaluated on MoGaze and GIMO, We need to train them from scratch. For a fair comparison, all training hyperparameters and settings were kept at their default values. All experiments were conducted in an Nvidia TITAN X GPU with 12GB memory using the PyTorch 1.7.1 framework. For both datasets, we applied the same training and hyperparameter settings, we jointly trained the gaze-motion fusion network and the noise prediction network using Adam optimization [30] with an initial learning rate of 0.0003 and the multi-step learning rate scheduler ($\gamma = 0.9$). The batch size was 32. We applied a standard diffusion process as proposed by [52] that degraded 1000 steps in the training and sampled 100 steps in the inference. We selected the Cosine scheduler [44] in the diffusion following HumanMAC [10]. The multi-modal ground truth threshold was set as 0.4 referred to previous work [4].

4.5 Quantitative Results

The quantitative results on MoGaze [33] and GIMO [66] are shown in Table 1. Overall, our model outperforms state-of-the-art methods on all accuracy metrics.

Table 1: Comparison of *GazeMoDiff* with the state-of-the-art methods on both MoGaze and GIMO. The best results are in bold and the second best results are underlined.

| | Results on MoGaze [33] | | | | | Results on GIMO [66] | | | | |
|----------------------|------------------------|------------------|------------------|--------------------|--------------------|----------------------|------------------|------------------|--------------------|--------------------|
| | APD \uparrow | ADE \downarrow | FDE \downarrow | MMADE \downarrow | MMFDE \downarrow | APD \uparrow | ADE \downarrow | FDE \downarrow | MMADE \downarrow | MMFDE \downarrow |
| <i>CVAE</i> [62] | <u>17.900</u> | 1.070 | 1.644 | 1.091 | 1.667 | <u>20.297</u> | 1.292 | 2.059 | 1.294 | 2.054 |
| <i>DLow</i> [62] | 22.277 | 0.807 | 1.261 | 0.840 | 1.274 | 24.538 | 1.084 | 1.688 | 1.090 | 1.687 |
| <i>BeLFusion</i> [4] | 17.099 | 0.899 | 1.306 | 0.908 | 1.313 | 17.959 | 0.840 | 1.220 | 0.845 | 1.221 |
| <i>HumanMAC</i> [10] | 11.867 | 0.732 | 1.089 | 0.779 | 1.144 | 15.040 | 0.815 | 1.121 | 0.821 | 1.118 |
| <i>Ours</i> | 14.037 | 0.622 | 0.923 | 0.632 | 0.930 | 14.907 | 0.749 | 1.021 | 0.754 | 1.026 |

Results on MoGaze. As shown in Table 1, *GazeMoDiff* achieves the lowest ADE, FDE, MMADE and MMFDE compared to all other methods, substantially surpassing the best state-of-the-art *HumanMAC*. For average displacement error (ADE), our method achieved an improvement of 15.03% (0.622 vs. 0.732) over *HumanMAC* [10]. On final displacement error (FDE), we obtain a 15.24% performance gain (0.923 vs. 1.089). These significant improvements demonstrate the value of jointly modeling historical gaze and joint movements for guiding human motion prediction. On multi-modal version accuracy metrics, our method improves the MMADE performance by 18.87% (0.632 vs. 0.779) and the MMFDE performance by 18.81% (0.930 vs. 1.144). The greater gains on the multi-modal metrics reveal our model is more capable of producing multimodal predictions aligned with the stochasticity of human nature. A Wilcoxon signed-rank test [59] indicates a statistically significant ADE difference ($p < 0.01$) between our proposed method and *HumanMAC*. Although diversity reduces due to gaze-guided predictions, compared to *DLow* with the highest APD, our method outperforms by 22.92%, 26.80%, 30.40% and 27.00% in terms of ADE, FDE, MMADE and MMFDE. It implies the predictions of *DLow* are not plausible so the diversity is meaningless somehow.

Results on GIMO. As shown in Table 1, our method *GazeMoDiff* is still superior among the state-of-the-art methods in all accuracy metrics. Our model lowers ADE by 9.20% compared to *HumanMAC* (0.815 to 0.749) and reduces FDE by 8.92% (1.212 to 1.021). On multi-modal accuracy, we attain 8.16% and 8.23% improvements in MMADE and MMFDE respectively. This demonstrates the strong generalisation ability of our approach to a new dataset. A Wilcoxon signed-rank test again showed a significant ADE difference ($p < 0.01$) versus *HumanMAC*. *DLow* also shows the highest APD values but particularly low accuracy on this dataset. Our method is superior to *DLow* by 30.9%, 39.51%, 30.83% and 39.18% in terms of ADE, FDE, MMADE and MMFDE, respectively. Additionally, previous work [55] pointed out that methods with high diversity metrics but low accuracy may suffer failure predictions. We will further discuss this phenomenon in Sect. 4.6.

4.6 Visualisation Analysis

We visualised the predicted pose in the future one second. We compared our method to the best diversity baseline, *DLow* [62], and the best accuracy approach, *HumanMAC* [10]. For each method, we randomly generate 10 predictions for comparison.

Visualisation results on the MoGaze dataset. We illustrated a representative visualisation from the MoGaze dataset [66] in Fig. 1. The observed motion sequence involves a turn to the right, and the ground truth pose shows a second later, this person continues the turn by about 90 degrees further to the right. We can observe that predictions of *HumanMAC* [10] and *DLow* [62] generally continue walking in the same forward direction as the observed last frame, failing to anticipate the full turning trajectory. The best predictions from baselines labelled in green also differ from the ground truth obviously. In contrast, by incorporating gaze guidance, our method is able to recognise that the person intends to keep turning right. As

a result, the best prediction from our method is precisely facing the true direction of motion in the ground truth and other predictions generally align with the ground truth. Due to the inherent uncertainty in predicting future speed, the body orientations of our predictions differ slightly from one another, reflecting the range of plausible orientation angles given the observed turning motion. In addition, generated poses are plausible without any angle distortions or strange limb lengths.

Visualisation results on the GIMO dataset. We also illustrated a typical visualisation from the GIMO dataset [66]. As depicted in Fig. 4, predictions from our methods are more similar to the ground truth. Furthermore, it is evident that all predictions from our method are generally realistic. In contrast, other methods yield predictions that include some implausible outcomes boxed in red. Corresponding with prior findings [10], we argued that some baselines like *DLow* achieved high APD but suffered from implausible cases. Despite the high APD calculated for these implausible prediction samples, they are meaningless and misleading for downstream tasks in fact. In contrast, predictions from our approach look natural with diversity.

4.7 Ablation Study

We conducted an ablation study to comprehensively analyse the individual contributions of various modules within our framework and evaluate the specific impact of incorporating gaze information.

We thoroughly assessed the performance of our model by comparing it to variants that exclude specific modules:

- *Ours_{w/o gat}*: Without spatio-temporal attention graph network
- *Ours_{w/o CA}*: Without cross attention in the noise predicting network
- *Ours_{w/o gaze}*: Without gaze as a virtual joint

Furthermore, we also compared our method to two diffusion baselines that incorporate gaze guidance.

- *BeLFusion_g*: We introduce gaze into *BeLFusion* by regarding gaze as a virtual joint as described in Sect. 4.1.
- *HumanMAC_g*: We introduce gaze into *HumanMac* in the same way.

As we report in Table 2, our model outperforms all variants and baseline methods with gaze. It reveals that each module integrated into our framework significantly contributes to the generation of accurate predictions. There are three notable findings worth discussing. 1) Compared to *GazeMoDiff*, the variant without gaze presents obviously lower accuracy in terms of both ADE and FDE, which demonstrates gaze information is effective. 2) Despite the variant without gaze not surpassing the performance *GazeMoDiff*, it notably outperforms other baselines without gaze, as presented in Table 1. This finding underscores the superiority of our proposed framework, whether or not gaze information is involved. 3)

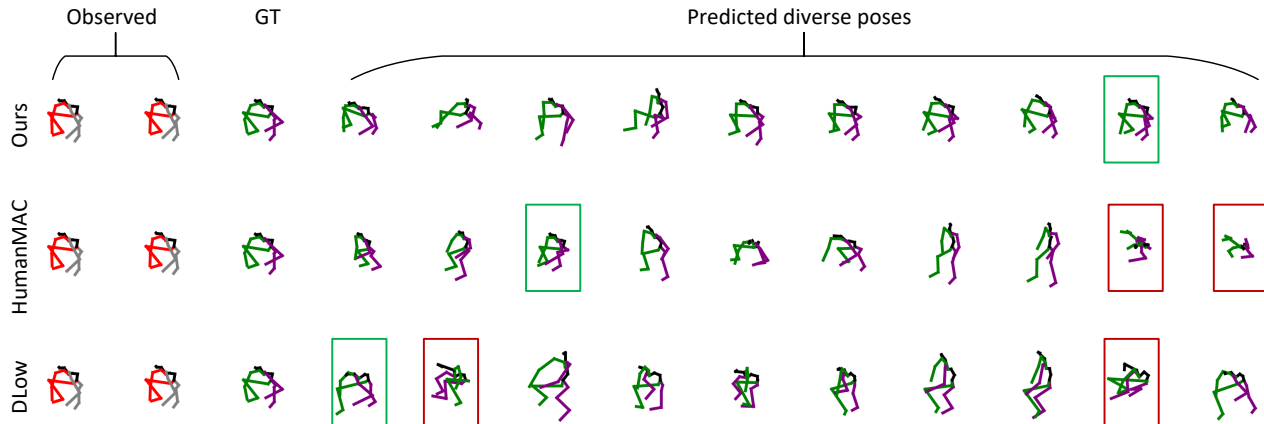


Figure 4: Motions in the future one second generated from different methods on the GIMO dataset [66] with best prediction boxed in green and implausible cases marked in red. Our method can generate realistic motions while other methods produce some implausible predictions.

Our approach outperforms both BeLFusion and HumanMAC which incorporate gaze information in terms of all accuracy metrics, showing the effective utilisation of gaze information to enhance overall performance.

Table 2: Ablation study on MoGaze [33]. The best results are in bold.

| | APD \uparrow | ADE \downarrow | FDE \downarrow | MMADE \downarrow | MMFDE \downarrow |
|--------------------------------|----------------|------------------|------------------|--------------------|--------------------|
| <i>Ours_{w/o gat}</i> | 11.088 | 0.678 | 1.002 | 0.691 | 1.011 |
| <i>Ours_{w/o CA}</i> | 13.252 | 0.676 | 0.957 | 0.686 | 0.966 |
| <i>Ours_{w/o gaze}</i> | 12.478 | 0.677 | 1.048 | 0.710 | 1.063 |
| <i>BeLFusion_g</i> | 15.711 | 0.654 | 1.018 | 0.659 | 1.012 |
| <i>HumanMAC_g</i> | 13.783 | 0.650 | 0.959 | 0.660 | 0.967 |
| <i>Ours</i> | 14.037 | 0.622 | 0.923 | 0.632 | 0.930 |

5 USER STUDY

To perform a comprehensive evaluation of the perceived realism of the generated samples, we conducted a user study to assess model performance based on human perception and intuition. Participants were tasked with ranking samples predicted by different motion forecasting models. By collecting subjective rankings directly from individuals, the user study provided an intuitive approach to evaluate aspects of the predictions that are challenging to assess objectively, such as naturalness, continuity, and the overall plausibility of the motions to a human observer.

5.1 Assessment Details

We randomly selected 6 sequences from the MoGaze dataset and 12 sequences from the GIMO dataset. The difference in the number of selections between the two datasets can be attributed to the difference in the variety of actions included. While the MoGaze dataset consists of only two actions, the GIMO dataset contains a larger number of diverse actions. We compared our method with the best accuracy baseline HumanMAC and the best diversity baseline DLow. Each method generated 10 predictions from random noise. The participants in our study were then instructed to rank these predictions based on overall realism, considering the following three key aspects:

- If these motions appeared **plausible**. Participants can identify any angle distortions, excessively short or long limbs, or poses that seem implausible.

- If these motions are **continuous**. Participants can check if there are any sudden or unreasonable changes during the whole motion.
- If these motions **align with the ground truth**. Participants can measure the similarity between each motion and ground truth.

The online questionnaire utilised in our study was created using the Jotform platform². The interface of our user study can be found in the supplementary material. A total of 23 individuals participated in our user study. This user study is approved by the University.

5.2 Evaluation

As shown in Table 3, it is evident that our method outperformed both DLow and HumanMAC, achieving the highest average ranking of 1.691. This indicates that our method was perceived as the most realistic by the participants overall. Remarkably, our method received the highest percentage of first-place rankings, with 49.52%, indicating that it was consistently ranked as the most realistic option. Additionally, it obtained a respectable 31.88% of second-place rankings. On the other hand, our method had the lowest percentage of third-place rankings at 18.60%, suggesting that it was least frequently perceived as the least realistic option. In comparison, DLow obtained the highest percentage of second-place rankings at 39.13%, but its first-place percentage was lower, at 26.33%. This reveals that DLow was less frequently considered the most realistic option but often ranked as the second most realistic. HumanMAC, on the other hand, had the highest percentage of third-place rankings at 46.60%, indicating that it was frequently perceived as the least realistic prediction. Moreover, its first and second-place percentages were the lowest among the three methods. To further validate our findings, we conducted a paired Wilcoxon signed-rank test, which revealed a statistically significant difference ($p < 0.01$) between our method and the second-best method, DLow, in terms of average rankings from all responses.

². <https://www.jotform.com/>

Table 3: Results of the on-line user study. The lower number of average rank is better.

| | Average Rank ↓ | 1st | 2nd | 3rd |
|-----------------|----------------|---------------|---------------|---------------|
| <i>DLow</i> | 2.082 | 26.33% | 39.13% | 34.54% |
| <i>HumanMAC</i> | 2.227 | 24.15% | 28.99% | 46.86% |
| <i>Ours</i> | 1.691 | 49.52% | 31.88% | 18.60% |

6 DISCUSSION

Our study marks a notable advancement in the emerging field of incorporating eye gaze cues for stochastic human motion prediction in VR research. We have successfully demonstrated the effectiveness of our proposed method in generating realistic human motion predictions.

Introducing gaze information. Introducing gaze as a modality allows the model to generate more realistic and goal-directed poses. Gaze cues provide valuable information about a person’s intentions and planned actions. In addition, the integration of gaze modality is highly practical. Modern VR headsets are equipped with built-in eye-tracking modules that can capture gaze data in real time. This means that gaze signals are readily available when using these devices, without the need for additional peripheral hardware. As presented in Table 1 and Table 2, gaze information indeed improves the accuracy of our model.

Potential for extension to other modalities. Our proposed approach, GazeMoDiff, has the potential to be extended to incorporate additional modalities beyond gaze. It serves as a multimodal human motion prediction framework, where various guidance information can be utilised to enhance the generation of reasonable motions. By incorporating modalities such as facial expressions, hand gestures, and physiological signals, the GazeMoDiff framework can be expanded to capture a more comprehensive range of cues for motion prediction. This multimodal approach can potentially lead to more contextually appropriate motion generation.

Limitations. We followed prior works [4, 10, 62] to select APD as our diversity metric. But measuring different prediction distances in this way is too simple and crude, and it is susceptible to extreme values. As shown in Fig. 4, we observed cases where HumanMAC [10] and DLow [62] were prone to produce distorted poses. Movement trends were diverse measured by a high APD But extremely implausible. For accurate metrics, ADE and FDE, the error is the smallest one among all predictions. Image an extreme case in a model that generated 1 very accurate prediction and 99 distorted and unrealistic predictions. It would be evaluated as a state-of-the-art model in the APD-ADE-FDE metrics system. However, the most of predictions are useless and misleading for downstream analysis. That is also why we evaluated further through visualisation analysis and user study. Besides, in our work, we predicted future motions by gaze and pose data. Gaze data is naturally available while pose needs to be captured by the wearable device. This may limit the application scenarios and be detrimental to the user experience.

Future work. In our future research endeavours, we aim to explore the potential for extending our framework to incorporate a variety of modalities, such as gaze, emotional text, physical parameters, and scene information. Existing datasets only consist of partial modalities like MoGaze [33] (Motion and Gaze), GIMO [66] (Motion and Gaze) and EBEDB (Gesture and Emotional label) [58]. It is worth exploring new datasets aggregating more modalities to enable more comprehensive multi-modal motion modeling and prediction. Additionally, to address the limitations associated with device dependency, we plan to develop a device-free approach. This approach would leverage different modalities, including gaze, motion, emotion, and scene information directly captured from video through learning-based estimation methods. By eliminating the need for users to wear specific devices or deploy complex sensors, this device-free method holds the potential to be applied in augmented

reality or mixed reality scenarios, enhancing user experience and portability. Furthermore, we recognise the need for improved metrics for stochastic human motion prediction. While metrics such as ADE, FDE, and APD have been widely used, there is room for further refinement and development of metrics that better capture the quality and usefulness of predicted motions. Enhancing the metrics will contribute to more accurate and comprehensive evaluations of human motion prediction methods.

7 CONCLUSION

In this work, we were the first to explore the effectiveness of eye gaze on generating realistic and diverse human motions. We proposed a novel gaze-guided diffusion model that first extracts spatio-temporal features from gaze and motion data and then uses these features to generate realistic human motions through a denoising diffusion process. Extensive experiments demonstrated that our method outperforms the state-of-the-art methods by a large margin in terms of prediction accuracy and an on-line user study validated that our method can generate motions that are more realistic than other methods. As such, our work makes an important step towards generating more realistic human motions for virtual agents and guides future work on cross-modal human behaviour generation.

REFERENCES

- [1] E. Aksan, M. Kaufmann, P. Cao, and O. Hilliges. A spatio-temporal transformer for 3d human motion prediction. In *2021 International Conference on 3D Vision (3DV)*, pp. 565–574. IEEE, 2021.
- [2] S. Aliakbarian, F. Saleh, L. Petersson, S. Gould, and M. Salzmann. Contextually plausible and diverse 3d human motion prediction. In *Proceedings of the IEEE/CVF International Conference on Computer Vision*, pp. 11333–11342, 2021.
- [3] M. Azmandian, T. Grechkin, M. Bolas, and E. Suma. Automated path prediction for redirected walking using navigation meshes. In *2016 IEEE Symposium on 3D User Interfaces (3DUI)*, pp. 63–66. IEEE, 2016.
- [4] G. Barquero, S. Escalera, and C. Palmero. Belfusion: Latent diffusion for behavior-driven human motion prediction. *arXiv preprint arXiv:2211.14304*, 2022.
- [5] E. Barsoum, J. Kender, and Z. Liu. Hp-gan: Probabilistic 3d human motion prediction via gan. In *Proceedings of the IEEE conference on computer vision and pattern recognition workshops*, pp. 1418–1427, 2018.
- [6] U. Bhattacharya, N. Rewkowski, A. Banerjee, P. Guhan, A. Bera, and D. Manocha. Text2gestures: A transformer-based network for generating emotive body gestures for virtual agents. In *2021 IEEE virtual reality and 3D user interfaces (VR)*, pp. 1–10. IEEE, 2021.
- [7] J. Butepage, M. J. Black, D. Kragic, and H. Kjellstrom. Deep representation learning for human motion prediction and classification. In *Proceedings of the IEEE conference on computer vision and pattern recognition*, pp. 6158–6166, 2017.
- [8] Z. Cao, H. Gao, K. Mangalam, Q.-Z. Cai, M. Vo, and J. Malik. Long-term human motion prediction with scene context. In *Computer Vision—ECCV 2020: 16th European Conference, Glasgow, UK, August 23–28, 2020, Proceedings, Part I 16*, pp. 387–404. Springer, 2020.
- [9] H. Chen, L. Wei, H. Liu, B. Shi, G. Zhang, and H. Zha. Mount: Learning 6dof motion prediction based on uncertainty estimation for delayed ar rendering. *IEEE Transactions on Visualization and Computer Graphics*, pp. 1–12, 2022. doi: 10.1109/TVCG.2022.3228807
- [10] L.-H. Chen, J. Zhang, Y. Li, Y. Pang, X. Xia, and T. Liu. Human-mac: Masked motion completion for human motion prediction. *arXiv preprint arXiv:2302.03665*, 2023.
- [11] S. Chen, P. Sun, Y. Song, and P. Luo. Diffusionnet: Diffusion model for object detection. *arXiv preprint arXiv:2211.09788*, 2022.
- [12] B. David-John, C. Peacock, T. Zhang, T. S. Murdison, H. Benko, and T. R. Jonker. Towards gaze-based prediction of the intent to interact in virtual reality. In *ACM Symposium on Eye Tracking Research and Applications*, pp. 1–7, 2021.

- [13] P. Dhariwal and A. Nichol. Diffusion models beat gans on image synthesis. *Advances in Neural Information Processing Systems*, 34:8780–8794, 2021.
- [14] Y. Du, R. Kips, A. Pumarola, S. Starke, A. Thabet, and A. Sanakouyeu. Avatars grow legs: Generating smooth human motion from sparse tracking inputs with diffusion model. In *Proceedings of the IEEE/CVF Conference on Computer Vision and Pattern Recognition*, pp. 481–490, 2023.
- [15] K. J. Emery, M. Zannoli, J. Warren, L. Xiao, and S. S. Talathi. Openneeds: A dataset of gaze, head, hand, and scene signals during exploration in open-ended vr environments. In *ACM Symposium on Eye Tracking Research and Applications*, pp. 1–7, 2021.
- [16] K. Fragkiadaki, S. Levine, P. Felsen, and J. Malik. Recurrent network models for human dynamics. In *Proceedings of the IEEE international conference on computer vision*, pp. 4346–4354, 2015.
- [17] N. M. Gamage, D. Ishtaweera, M. Weigel, and A. Withana. So predictable! continuous 3d hand trajectory prediction in virtual reality. In *The 34th Annual ACM Symposium on User Interface Software and Technology*, pp. 332–343, 2021.
- [18] P. Ghosh, J. Song, E. Aksan, and O. Hilliges. Learning human motion models for long-term predictions. In *2017 International Conference on 3D Vision (3DV)*, pp. 458–466. IEEE, 2017.
- [19] A. Gopalakrishnan, A. Mali, D. Kifer, L. Giles, and A. G. Ororbia. A neural temporal model for human motion prediction. In *Proceedings of the IEEE/CVF Conference on Computer Vision and Pattern Recognition*, pp. 12116–12125, 2019.
- [20] J. Ho, A. Jain, and P. Abbeel. Denoising diffusion probabilistic models. *Advances in neural information processing systems*, 33:6840–6851, 2020.
- [21] J. Ho, T. Salimans, A. Gritsenko, W. Chan, M. Norouzi, and D. J. Fleet. Video diffusion models. *arXiv preprint arXiv:2204.03458*, 2022.
- [22] J. E. Holm. *Collision prediction and prevention in a simultaneous multi-user immersive virtual environment*. PhD thesis, Miami University, 2012.
- [23] X. Hou, J. Zhang, M. Budagavi, and S. Dey. Head and body motion prediction to enable mobile vr experiences with low latency. In *2019 IEEE Global Communications Conference (GLOBECOM)*, pp. 1–7. IEEE, 2019.
- [24] Z. Hu, A. Bulling, S. Li, and G. Wang. Ehtask: Recognizing user tasks from eye and head movements in immersive virtual reality. *IEEE Transactions on Visualization and Computer Graphics*, 2021.
- [25] Z. Hu, A. Bulling, S. Li, and G. Wang. Fixationnet: Forecasting eye fixations in task-oriented virtual environments. *IEEE Transactions on Visualization and Computer Graphics*, 27(5):2681–2690, 2021.
- [26] Z. Hu, S. Li, C. Zhang, K. Yi, G. Wang, and D. Manocha. Dgaze: Cnn-based gaze prediction in dynamic scenes. *IEEE Transactions on Visualization and Computer Graphics*, 26(5):1902–1911, 2020.
- [27] Z. Hu, C. Zhang, S. Li, G. Wang, and D. Manocha. Sgaze: A data-driven eye-head coordination model for realtime gaze prediction. *IEEE transactions on visualization and computer graphics*, 25(5):2002–2010, 2019.
- [28] D. K. Jain, M. Zareapoor, R. Jain, A. Kathuria, and S. Bachhety. Ganposer: an improvised bidirectional gan model for human motion prediction. *Neural Computing and Applications*, 32(18):14579–14591, 2020.
- [29] Y. Kim, J. An, M. Lee, and Y. Lee. An activity-embedding approach for next-activity prediction in a multi-user smart space. In *2017 IEEE International Conference on Smart Computing (SMARTCOMP)*, pp. 1–6. IEEE, 2017.
- [30] D. P. Kingma and J. Ba. Adam: A method for stochastic optimization. *arXiv preprint arXiv:1412.6980*, 2014.
- [31] F. Koochaki and L. Najafzadeh. Predicting intention through eye gaze patterns. In *2018 IEEE Biomedical Circuits and Systems Conference (BioCAS)*, pp. 1–4. IEEE, 2018.
- [32] R. Kothari, Z. Yang, C. Kanan, R. Bailey, J. B. Pelz, and G. J. Diaz. Gaze-in-wild: A dataset for studying eye and head coordination in everyday activities. *Scientific reports*, 10(1):2539, 2020.
- [33] P. Kratzer, S. Bihlmaier, N. B. Midlagajni, R. Prakash, M. Toussaint, and J. Mainprice. Mogaze: A dataset of full-body motions that includes workspace geometry and eye-gaze. *IEEE Robotics and Automation Letters*, 6(2):367–373, 2020.
- [34] J. N. Kundu, M. Gor, and R. V. Babu. Bihmp-gan: Bidirectional 3d human motion prediction gan. In *Proceedings of the AAAI conference on artificial intelligence*, vol. 33, pp. 8553–8560, 2019.
- [35] M. Li, S. Chen, Y. Zhao, Y. Zhang, Y. Wang, and Q. Tian. Multiscale spatio-temporal graph neural networks for 3d skeleton-based motion prediction. *IEEE Transactions on Image Processing*, 30:7760–7775, 2021.
- [36] Q. Li, G. Chalvatzaki, J. Peters, and Y. Wang. Directed acyclic graph neural network for human motion prediction. In *2021 IEEE International Conference on Robotics and Automation (ICRA)*, pp. 3197–3204. IEEE, 2021.
- [37] Z. Li, Y. Zhou, S. Xiao, C. He, Z. Huang, and H. Li. Auto-conditioned recurrent networks for extended complex human motion synthesis. *arXiv preprint arXiv:1707.05363*, 2017.
- [38] T. Ma, Y. Nie, C. Long, Q. Zhang, and G. Li. Progressively generating better initial guesses towards next stages for high-quality human motion prediction. In *Proceedings of the IEEE/CVF Conference on Computer Vision and Pattern Recognition*, pp. 6437–6446, 2022.
- [39] W. Mao, M. Liu, and M. Salzmann. Generating smooth pose sequences for diverse human motion prediction. In *Proceedings of the IEEE/CVF International Conference on Computer Vision*, pp. 13309–13318, 2021.
- [40] W. Mao, M. Liu, M. Salzmann, and H. Li. Learning trajectory dependencies for human motion prediction. In *Proceedings of the IEEE/CVF International Conference on Computer Vision*, pp. 9489–9497, 2019.
- [41] J. Martinez, M. J. Black, and J. Romero. On human motion prediction using recurrent neural networks. In *Proceedings of the IEEE conference on computer vision and pattern recognition*, pp. 2891–2900, 2017.
- [42] A. Martínez-González, M. Villamizar, and J.-M. Odobez. Pose transformers (potr): Human motion prediction with non-autoregressive transformers. In *Proceedings of the IEEE/CVF International Conference on Computer Vision*, pp. 2276–2284, 2021.
- [43] A. Nichol, P. Dhariwal, A. Ramesh, P. Shyam, P. Mishkin, B. McGrew, I. Sutskever, and M. Chen. Glide: Towards photorealistic image generation and editing with text-guided diffusion models. *arXiv preprint arXiv:2112.10741*, 2021.
- [44] A. Q. Nichol and P. Dhariwal. Improved denoising diffusion probabilistic models. In *International Conference on Machine Learning*, pp. 8162–8171. PMLR, 2021.
- [45] A. Ramesh, P. Dhariwal, A. Nichol, C. Chu, and M. Chen. Hierarchical text-conditional image generation with clip latents. *arXiv preprint arXiv:2204.06125*, 1(2):3, 2022.
- [46] K. Rasul, C. Seward, I. Schuster, and R. Vollgraf. Autoregressive denoising diffusion models for multivariate probabilistic time series forecasting. In *International Conference on Machine Learning*, pp. 8857–8868. PMLR, 2021.
- [47] R. Rombach, A. Blattmann, D. Lorenz, P. Esser, and B. Ommer. High-resolution image synthesis with latent diffusion models. In *Proceedings of the IEEE/CVF Conference on Computer Vision and Pattern Recognition*, pp. 10684–10695, 2022.
- [48] S. Saadatnejad, A. Rasekh, M. Mofayez, Y. Medghalchi, S. Rajabzadeh, T. Mordan, and A. Alahi. A generic diffusion-based approach for 3d human pose prediction in the wild. In *2023 IEEE International Conference on Robotics and Automation (ICRA)*, pp. 8246–8253. IEEE, 2023.
- [49] L. Sidenmark and H. Gellersen. Eye, head and torso coordination during gaze shifts in virtual reality. *ACM Transactions on Computer-Human Interaction (TOCHI)*, 27(1):1–40, 2019.
- [50] L. Sidenmark and H. Gellersen. Eye&head: Synergetic eye and head movement for gaze pointing and selection. In *Proceedings of the 2019 ACM Symposium on User Interface Software and Technology*, pp. 1161–1174, 2019.
- [51] L. Sidenmark, D. Mardanbegi, A. R. Gomez, C. Clarke, and H. Gellersen. Bimodalgaze: Seamlessly refined pointing with gaze and filtered gestural head movement. In *ACM Symposium on Eye Tracking Research and Applications*, pp. 1–9, 2020.
- [52] J. Song, C. Meng, and S. Ermon. Denoising diffusion implicit models. *arXiv preprint arXiv:2010.02502*, 2020.
- [53] Q. Sun, A. Patney, L.-Y. Wei, O. Shapira, J. Lu, P. Asente, S. Zhu, M. McGuire, D. Luebke, and A. Kaufman. Towards virtual reality

- infinite walking: dynamic saccadic redirection. *ACM Transactions on Graphics (TOG)*, 37(4):1–13, 2018.
- [54] Y. Tashiro, J. Song, Y. Song, and S. Ermon. Cstdi: Conditional score-based diffusion models for probabilistic time series imputation. *Advances in Neural Information Processing Systems*, 34:24804–24816, 2021.
- [55] G. Tevet, S. Raab, B. Gordon, Y. Shafir, D. Cohen-Or, and A. H. Bermano. Human motion diffusion model. *arXiv preprint arXiv:2209.14916*, 2022.
- [56] A. Vaswani, N. Shazeer, N. Parmar, J. Uszkoreit, L. Jones, A. N. Gomez, Ł. Kaiser, and I. Polosukhin. Attention is all you need. *Advances in neural information processing systems*, 30, 2017.
- [57] P. Veličković, G. Cucurull, A. Casanova, A. Romero, P. Lio, and Y. Bengio. Graph attention networks. *arXiv preprint arXiv:1710.10903*, 2017.
- [58] E. Volkova, S. De La Rosa, H. H. Bühlhoff, and B. Mohler. The mpi emotional body expressions database for narrative scenarios. *PloS one*, 9(12):e113647, 2014.
- [59] F. Wilcoxon. Individual comparisons by ranking methods. In *Breakthroughs in Statistics: Methodology and Distribution*, pp. 196–202. Springer, 1992.
- [60] J. Wyatt, A. Leach, S. M. Schmon, and C. G. Willcocks. Anoddpn: Anomaly detection with denoising diffusion probabilistic models using simplex noise. In *Proceedings of the IEEE/CVF Conference on Computer Vision and Pattern Recognition*, pp. 650–656, 2022.
- [61] J. Xu, X. Wang, W. Cheng, Y.-P. Cao, Y. Shan, X. Qie, and S. Gao. Dream3d: Zero-shot text-to-3d synthesis using 3d shape prior and text-to-image diffusion models. *arXiv preprint arXiv:2212.14704*, 2022.
- [62] Y. Yuan and K. Kitani. Dlow: Diversifying latent flows for diverse human motion prediction. In *Computer Vision—ECCV 2020: 16th European Conference, Glasgow, UK, August 23–28, 2020, Proceedings, Part IX 16*, pp. 346–364. Springer, 2020.
- [63] W. H. Zangemeister and L. Stark. Gaze latency: variable interactions of head and eye latency. *Experimental Neurology*, 75(2):389–406, 1982.
- [64] L. Zhang and M. Agrawala. Adding conditional control to text-to-image diffusion models. *arXiv preprint arXiv:2302.05543*, 2023.
- [65] M. Zhang, Z. Cai, L. Pan, F. Hong, X. Guo, L. Yang, and Z. Liu. Motiondiffuse: Text-driven human motion generation with diffusion model. *arXiv preprint arXiv:2208.15001*, 2022.
- [66] Y. Zheng, Y. Yang, K. Mo, J. Li, T. Yu, Y. Liu, C. K. Liu, and L. J. Guibas. Gimo: Gaze-informed human motion prediction in context. In *European Conference on Computer Vision*, pp. 676–694. Springer, 2022.